

Nanocalorimetric evidence for nematic superconductivity in the doped topological insulator $\text{Sr}_{0.1}\text{Bi}_2\text{Se}_3$


Kristin Willa,^{1,*} Roland Willa,¹ Kok Wee Song,¹ G. D. Gu,² John A. Schneeloch,^{2,3} Ruidan Zhong,^{2,4} Alexei E. Koshelev,¹ Wai-Kwong Kwok,¹ and Ulrich Welp¹

¹Materials Science Division, Argonne National Laboratory, Lemont, Illinois 60439, USA

²Condensed Matter Physics and Materials Science Department, Brookhaven National Laboratory, Upton, New York 11793, USA

³Department of Physics and Astronomy, Stony Brook University, Stony Brook, New York 11794, USA

⁴Department of Materials Science and Engineering, Stony Brook University, Stony Brook, New York 11794, USA

 (Received 27 July 2018; revised manuscript received 15 October 2018; published 19 November 2018)

Spontaneous rotational-symmetry breaking in the superconducting state of doped Bi_2Se_3 has attracted significant attention as an indicator for topological superconductivity. In this paper, high-resolution calorimetry of the single-crystal $\text{Sr}_{0.1}\text{Bi}_2\text{Se}_3$ provides unequivocal evidence of a twofold rotational symmetry in the superconducting gap by a *bulk thermodynamic* probe, a fingerprint of nematic superconductivity. The extremely small specific heat anomaly resolved with our high-sensitivity technique is consistent with the material's low carrier concentration proving bulk superconductivity. The large basal-plane anisotropy of H_{c2} ($\Gamma_{\text{exp}} = 3.5$) is attributed to a nematic phase of a two-component topological gap structure $\eta = (\eta_1, \eta_2)$ and caused by a symmetry-breaking energy term $\delta(|\eta_1|^2 - |\eta_2|^2)T_c$. A quantitative analysis of our data excludes more conventional sources of this twofold anisotropy and provides an estimate for the symmetry-breaking strength $\delta \approx 0.1$, a value that points to an onset transition of the second order parameter component below 2 K.

DOI: [10.1103/PhysRevB.98.184509](https://doi.org/10.1103/PhysRevB.98.184509)

I. INTRODUCTION

The prospect of fault-tolerant quantum computing based on the non-Abelian braiding properties of Majorana fermions has generated enormous interest in the synthesis and study of topological superconductors [1–4]. Currently, two paths towards topological superconductivity are being pursued: proximity-induced topological states at the *interface* between a conventional superconductor and a topological insulator or a strong spin-orbit coupled semiconductor [5–7], respectively, or by doping-induced superconductivity in *bulk* topological insulators [8,9]. Among the doped topological insulators, $M\text{Bi}_2\text{Se}_3$ (with $M = \text{Cu}$ [10], Nb [11], Sr [12]) have attracted considerable interest since they display a phenomenology—the spontaneous emergence of a twofold in-plane anisotropy of various superconducting quantities in a threefold in-plane crystal structure [13–16] and evidence for a nodal gap [17,18]—that is consistent with a topological state. Several theoretical works [19–21] propose a two-component superconducting order parameter $\eta = (\eta_1, \eta_2)$ of E_u symmetry for this class of materials. This order parameter by itself does not lead to a twofold in-plane symmetry; yet the asymmetric coupling of the two order parameter components, analogous to the case of the unconventional superconductor UPt_3 [22], causes a symmetry breaking. For the doped Bi_2Se_3 , a coupling to the strain field $\delta(|\eta_1|^2 - |\eta_2|^2)T_c$ has been proposed to induce the nematic state, where the coupling strength is quantified by the phenomenological parameter δ [21].

The twofold H_{c2} anisotropy in $\text{Sr}_x\text{Bi}_2\text{Se}_3$ has been studied using several complementary approaches, including magnetotransport [23], transport under pressure [24], Corbino geometry [25], and magnetization [26]. While confirming the twofold rotational anisotropy, these studies also point towards an isotropic response in the *normal state*, i.e., excluding conventional sources of anisotropy such as an elliptic Fermi surface, structural inhomogeneities, or magnetic impurities. A

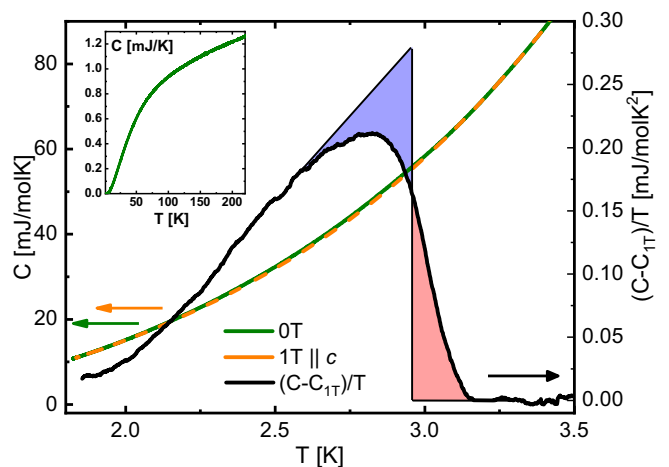


FIG. 1. Zero-field heat capacity measurement of $\text{Sr}_{0.1}\text{Bi}_2\text{Se}_3$ from room temperature down to 1.8 K (green, inset) and a closeup near the superconducting transition (main figure). The latter becomes visible only after subtraction of a normal-state background (orange). The subtracted curve (black, and normalized by T) reveals a small relative specific heat jump $\Delta C/C \sim 10^{-2}$; yet compatible with bulk superconductivity.

*Corresponding author: kristin.willa@kit.edu

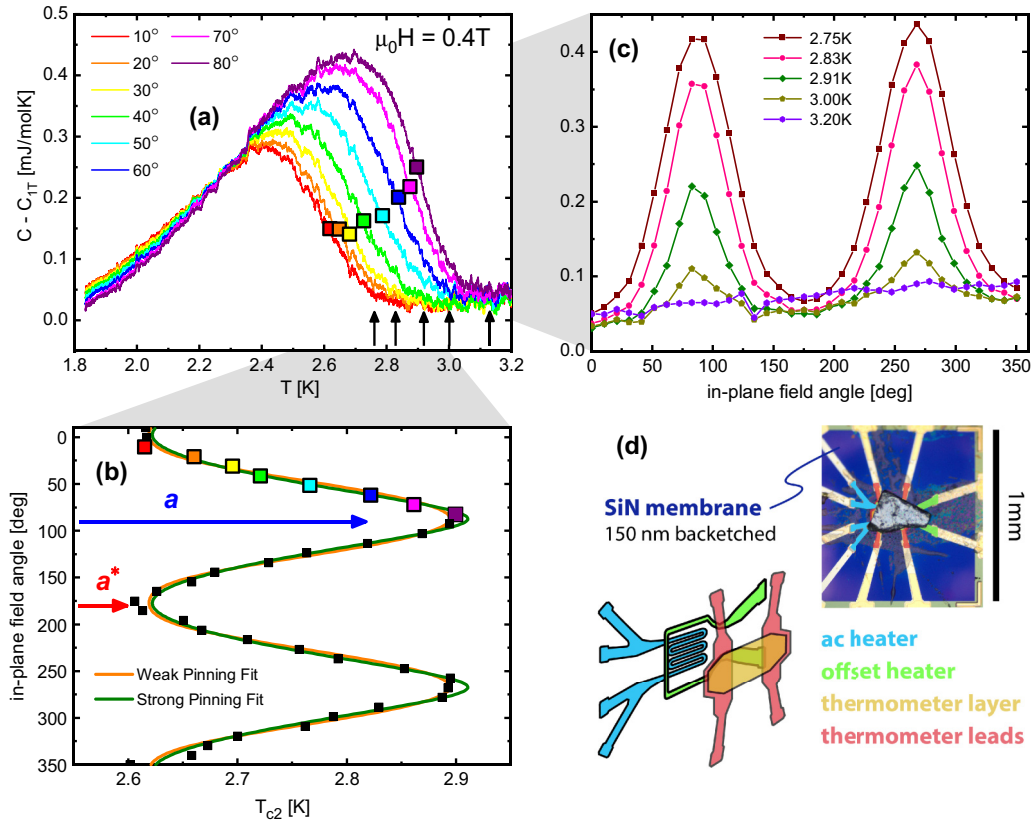


FIG. 2. (a) Calorimetric scans—taken at fixed magnetic field strength $\mu_0 H = 0.4$ T—for different field orientations in the basal plane. (b) Angular dependence of the upper critical temperature $T_{c2}(\theta)$, where each point results from a full specific heat scan [see colored squares in (a)]. $T_{c2}(\theta)$ assumes a maximal (minimal) value 2.9 K (2.6 K) along the a (a^*) direction. Weak and strong pinning fits are discussed in the main text. (c) Appearance of anisotropy in the specific heat when the sample is cooled through the superconducting transition. Each curve corresponds to a cut at constant temperature [indicated by vertical arrows in (a)]. The absence of an anisotropy above T_c is consistent with earlier works on magnetization and magnetotransport. (d) Microscope image of $\text{Sr}_{0.1}\text{Bi}_2\text{Se}_3$ single crystal on the nanocalorimetric platform, and platform architecture.

specific heat study [23] concluded that no structural transition is breaking the crystalline symmetry. However, this measurement did not yield a discernible specific heat anomaly at the superconducting transition. Whereas the twofold symmetry has been demonstrated beyond any doubt, pressing open questions remain, e.g., on the selection of the nematic direction and the origin of the strain field. Determining the strength of this field δ is essential in understanding the nematic state in these compounds and thus an important step on the way to find topological superconductivity.

II. EXPERIMENT AND RESULTS

In this paper we report calorimetric measurements on $\text{Sr}_{0.1}\text{Bi}_2\text{Se}_3$ single crystals synthesized by the melt-growth technique [25] and show the first observation of a clear step of 0.28 mJ/mol K^2 in the specific heat at the superconducting transition near 3 K. The step height, albeit small, is in agreement with estimates based on magnetization measurements and the electronic band structure. The specific heat measurements do not reveal a double transition as seen for instance in UPt_3 [22] establishing boundaries on the coupling strength to a symmetry-breaking strain field of $\delta > 0.1$. In conjunction with a theoretical analysis of the upper critical field of a

superconductor with a two-component order parameter our measurements reveal that $\text{Sr}_{0.1}\text{Bi}_2\text{Se}_3$ is in the strong-coupling regime accompanied by a temperature-independent in-plane anisotropy.

The ac specific heat is measured on a SiN calorimetric membrane [27,28], and the experiment is controlled with a SynkTek MCL1-540 multichannel lock-in system. A small ($200 \times 300 \times 25$ μm^3) platelet-shaped single crystal is mounted on the nanocalorimeter platform with apiezon grease, and inserted into a 1-1-9T three axis superconducting vector magnet. The c axis of the sample is aligned with the magnet's 9T (or z) direction.

The measured heat capacity (chip background subtracted) is featureless and does not reveal any indication of a structural transition occurring during cool-down from room temperature (Fig. 1). Even the superconducting transition is not apparent in the raw data (see main panel). However, the superconducting transition becomes visible after subtracting normal-state data C_{1T}/T (obtained by applying 1 T along the c axis, see Ref. [26]) from the zero-field curve. The transition temperature—as extracted from an entropy conserving construction—amounts to $T_c = 2.95$ K. The step height at the transition of 0.28 mJ/mol K^2 corresponds to about 1% of the total signal and is ~ 50 times smaller than in a

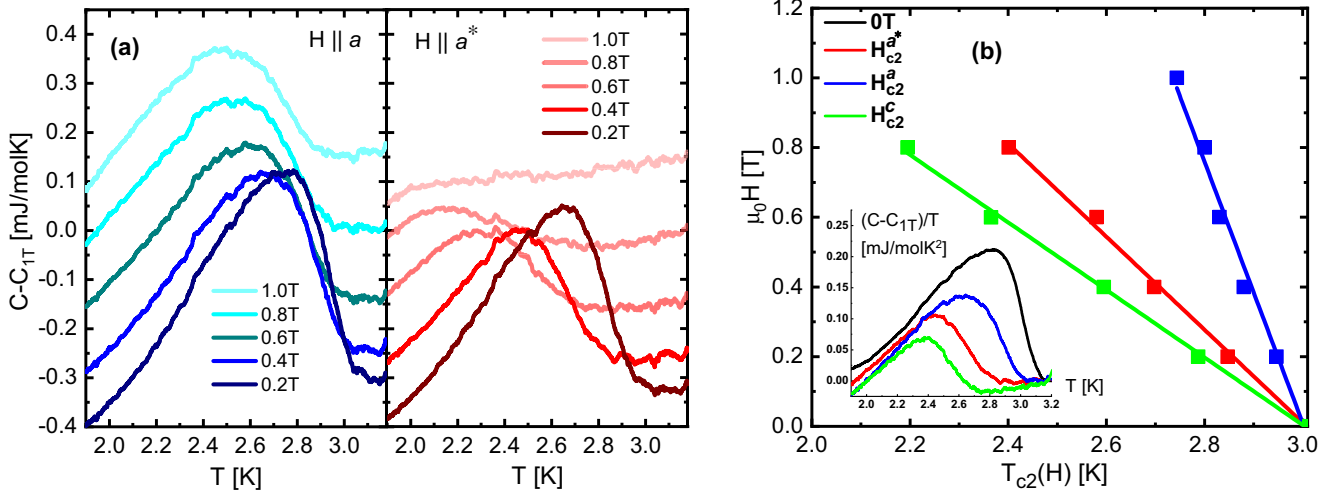


FIG. 3. (a) Calorimetric scans along the basal principal axes for various field strengths (curves are arbitrarily offset for better visibility), see blue and red arrows in Fig. 2 (b), reveal a robust superconducting order along a and a less robust one along a^* . (b) The H_{c2} phase boundary—shown for all three principal axes—features a temperature-independent anisotropy $\Gamma_{\text{exp}} = 3.5$ between the two basal-plane upper critical fields. A comparison between the 0.4 T calorimetric scans along the three crystallographic directions (blue, red, green) and the zero field specific heat (black) is given in the inset.

conventional superconductor (e.g., lead). Superconducting shielding fractions of 70% have been reported [29] while thermodynamic evidence was missing so far. We now want to verify the consistency of the measured magnitude of ΔC with other superconducting and normal state parameters of the material to show bulk superconductivity. The relation $\Delta C = (T_c/4\pi)(\partial H_c/\partial T)|_{T_c}$ —originally derived by Rutgers [30]—provides an estimate for the jump in the specific heat in terms of the slope of the critical field H_c . Here ΔC is given in $\text{erg cm}^{-3} \text{ K}^{-1}$. Substituting $H_c = H_{c2}/\kappa\sqrt{2}$ and using the relation $\partial M/\partial T = -(8\pi\beta_A\kappa^2)^{-1}(\partial H_{c2}/\partial T)_{T_c}$ [with $\beta_A \approx 1.16$] derived [31] for a large Ginzburg-Landau parameter κ , we arrive at

$$\Delta C/T_c = -\beta_A(\partial M/\partial T)(\partial H_{c2}/\partial T)_{T_c}. \quad (1)$$

These relations remain valid for a multicomponent order parameter in the linear regime near T_c . With the slope $\partial M/\partial T = 2.5 \times 10^{-3} \text{ emu/cm}^3 \text{ K}$ reported in Ref. [26] for single crystals from the same synthesis batch and the slope $\partial H_{c2}/\partial T = -10 \text{ kG/K}$ determined below, we arrive at an estimate $\Delta C/T_c = 0.2 \text{ mJ/mol K}^2$ which agrees well with the observed value and demonstrates that different measured parameters are thermodynamically consistent. Within single-band weak-coupling BCS theory [32], the jump in the specific heat satisfies the relation $\Delta C/T_c = 1.43\gamma$, with the Sommerfeld coefficient $\gamma = (\pi^2/2)k_B^2 n/\epsilon_F$ expressed in terms of the charge carrier density n and the Fermi energy ϵ_F . We use reported values for n and ϵ_F obtained from Seebeck and Hall effect measurements [33] to evaluate the Sommerfeld coefficient. These estimates provide a value for $\Delta C/T_c = 0.42 \text{ mJ/mol K}^2$, again close to our measured value. With these estimates we exclude the scenario of a tiny superconducting volume fraction.

The in-plane anisotropy of the specific heat is studied by applying a field of fixed strength (0.4 T) in the plane normal to the crystallographic c axis and by rotating it in steps of

10 deg. At each step we measure the specific heat upon cooling through the transition from 3.2 down to 1.8 K. A set of scans is shown in Fig. 2 [with the normal state (1 T along the c axis) curve already subtracted]. The transition temperature and magnitude clearly depend on the in-plane field orientation. For each field angle, the upper critical temperature $T_{c2}(\theta)$ is extracted from the inflection point¹ in $[C(T) - C_{1T}(T)]/T$, see Fig. 2(a). As a function of θ , the upper critical temperature shows a strong twofold in-plane anisotropy, with $T_{c2}^{\text{max}} = 2.9 \text{ K}$ and $T_{c2}^{\text{min}} = 2.6 \text{ K}$ along two directions separated by 90° . These axes have previously been identified as the crystallographic a and a^* directions, respectively [23,26]. Focusing on the principal axes, we performed more detailed measurements of the superconducting phase boundary with field strengths between 0.2 and 1 T. From the specific heat curves along the two extremal in-plane directions, shown in Fig. 3(a), the H_{c2} phase boundary can be determined, see Fig. 3(b). The in-plane anisotropy of H_{c2} amounts to $\Gamma_{\text{exp}} = H_{c2}^a/H_{c2}^{a^*} = 3.5$ and is independent of the temperature (within the studied field range). For completeness the c -axis phase boundary is also determined; a direct comparison of the calorimetric curves for these three directions (at 0.4 T) is shown in Fig. 3(b). We note that in the normal state the specific heat is isotropic in the plane as evidenced by the 3.2 K data in Fig. 2(c). We thus exclude normal-state properties

¹It shall be noted here that a more rigorous definition of the transition temperature involves an entropy conserving construction. The latter however requires an accurate determination of the specific heat away from the transition temperature, a criterion that is not systematically met for all angles. Comparing both methods (where applicable) reveals a small shift by $\sim 0.05 \text{ K}$ in T_c and a negligible difference in its angular dependence.

as the cause of in-plane anisotropy of H_{c2} . An alternative explanation for an anisotropic H_{c2} in doped Bi_2Se_3 was laid out by Venderbos and co-workers [21] (earlier work on UPt_3 goes back to Agterberg *et al.* [34,35]) and invokes a two-component order parameter $\eta = (\eta_1, \eta_2)$. The order parameter is usually treated by the Ginzburg-Landau (GL) formalism, where the linearized GL equations near H_{c2} read

$$\begin{aligned} (T_{c0} - T)\eta_a &= J(D_x^2 + D_y^2)\eta_a + K D_z^2 \eta_a - \delta T_{c0} \tau_3^{ab} \eta_b \\ &\times \mu J[(D_x^2 - D_y^2)\tau_3^{ab} + (D_x D_y - D_y D_x)\tau_1^{ab}]\eta_b, \end{aligned} \quad (2)$$

with T_{c0} the bare transition temperature (when $\delta = 0$), $D_\alpha = -i\partial_\alpha - 2eA_\alpha$ ($\alpha = x, y, z$) are gauge-invariant gradients, \mathbf{A} is the electromagnetic vector potential, τ_α are the Pauli matrices, and $\hbar = 1$. Summation is done over double indices. In this picture, a twofold anisotropy can exist only if both parameters δ (coupling the order parameters to the strain), and μ (ratio between GL parameters for the isotropic and mixed gradient terms) are nonvanishing. A finite δ (we take $\delta > 0$ for definition) shifts the mean-field transition temperature of the component η_1 to $T_c \equiv T_{c0}(1 + \delta)$ and that of η_2 to $T_{c0}(1 - \delta)$, respectively. It takes a substantial effort and limiting assumptions to derive the angular dependence of $H_{c2}(\theta)$. Several such limits have been considered in preceding works [16,21]. However, the anisotropy ratio $\Gamma = H_{c2}^{\max}/H_{c2}^{\min}$ between the maximal and minimal field directions can be solved without any restriction on the magnitude of δ and μ , see the Supplemental Material [36]. It turns out that for sufficiently large $\delta > \delta_c$, with δ_c determined by $2\delta_c/(1 + \delta_c) = (1 - T/T_c)\{1 - [(1 - \mu)/(1 + \mu)]^{1/2}\}$, the anisotropy ratio reads $\Gamma_{>} = [(1 + \mu)/(1 - \mu)]^{1/2}$ and is independent of both δ and the temperature. Below that bound, the ratio reads $\Gamma_{<} = 1 + 2\delta/[(1 + \delta)(1 - T/T_c) - 2\delta]$, independent of μ and explicitly temperature dependent.

Our experiment clearly indicates a temperature-independent anisotropy, hence excluding the scenario for very small $\delta \ll \delta_c$. An implicit equation for $H_{c2}(\theta)$ has been derived for moderate δ ($\lesssim 1 - \mu$), see Eq. (108) in the Supplementary Material of Ref. [21]. A numerical fit (weak pinning fit, see Fig. 2) to our data shows a very good agreement, see Fig. 2(b), and provides an estimate for $\mu = 0.82$ and $\delta = 0.09$. These values imply that the appearance of the second (suppressed) order parameter near $T_{c,2} \approx T_c(1 - \delta)/(1 + \delta) \sim 2.5$ K causes a second discontinuity in the specific heat; a feature that is not resolved in the data.

For UPt_3 —an extensively studied unconventional heavy-Fermion superconductor with a two-component order parameter [22]—it is believed that weak antiferromagnetism lifts the degeneracy of the order parameter components giving rise to two distinct zero-field transitions in the specific heat split apart by 60 mK [37–40]. A phenomenological GL analysis [41] shows that the ratio of the specific heat jumps at the two transition temperatures (T_c and $T_{c,2}$) involves the phenomenological parameters associated with the quartic terms in the GL free energy. As a result, no parametric

smallness is imposed on the second calorimetric discontinuity. A thermodynamic analysis [42,43] reveals that the amplitude ratio of the specific heat anomalies depends on the slopes of the phase boundaries separating the normal state and the various order parameter configurations, respectively. Here again, unless these boundaries are very steep or horizontal, the amplitudes of the specific heat anomalies are expected to be of the same order of magnitude. In the case of $\text{Sr}_{0.1}\text{Bi}_2\text{Se}_3$, only the normal state boundary is currently known. Noting the absence of a second discontinuity in the specific heat, our results therefore imply that δ is large, shifting the second transition to low temperatures. Then, by identifying the measured anisotropy of 3.5 with $\Gamma_{>}$, a value of $\mu = 0.85$ and a lower bound for $\delta > \delta_c \approx 0.11$ are obtained. For very large $\delta \gg \delta_c$, the order parameter is pinned to the pure form $\eta = (\eta_1, 0)$ at H_{c2} (along any angle), and a simple effective-mass-like dependence $H_{c2}^{\max}[\cos^2 \vartheta + \Gamma^2 \sin^2 \vartheta]^{-1/2}$ can be derived [16] (here $\vartheta \equiv \theta - \theta_{\max}$ is the angle measured away from the maximal H_{c2} direction). A corresponding (strong pinning) fit to our experimental result is shown in Fig. 2(b) producing the same fit quality as for the weaker pinning field.

We have investigated the anisotropic response of the superconducting state of $\text{Sr}_{0.1}\text{Bi}_2\text{Se}_3$ through high-precision calorimetric measurements. From our work we conclude that (i) the normal state has an isotropic basal plane, (ii) no structural transition is observed down to 1.8 K, (iii) the jump in the specific heat at T_c is small, consistent with the behavior of the magnetization and with a very low electron concentration, and (iv) the basal-plane anisotropy of H_{c2} is large, i.e., $\Gamma_{\text{exp}} = 3.5$ and temperature independent. The prevailing theoretical explanation for this anisotropy is based [21] on a two-component gap function realizing a nematic superconducting state due to possibly strain-induced symmetry breaking. Within this framework, the experimental data allows (v) to estimate the ratio $\mu = 0.85$ between the GL parameters for the isotropic and mixed gradient terms, and (vi) most importantly provides a lower bound for the symmetry-breaking strength $\delta > \delta_c \approx 0.1$, the parameter that causes the decoupling of the two order parameters.

Whereas the appearance of the order parameter's second component is expected to leave its trace in calorimetry, see Refs. [22,37] on UPt_3 , we surmise this feature to be below 1.8 K giving another indication of a strong pinning field δ . These results open the door for further studies looking for the proof to topological superconductivity in the material class of the doped Bi_2Se_3 .

ACKNOWLEDGMENTS

We cordially thank Matthew P. Smylie for fruitful discussions. This work was supported by the U.S. Department of Energy, Office of Science, Basic Energy Sciences, Materials Sciences and Engineering Division. K.W. and R.W. acknowledge support from the Swiss National Science Foundation through the Postdoc Mobility program. Work at Brookhaven is supported by the Office of Basic Energy Sciences, U.S. Department of Energy under Contract No. DE-SC0012704.

- [1] C. Nayak, S. H. Simon, A. Stern, M. Freedman, and S. Das Sarma, Non-Abelian anyons and topological quantum computation, *Rev. Mod. Phys.* **80**, 1083 (2008).
- [2] Z. Merali, Quantum computing: The power of discord, *Nature (London)* **474**, 24 (2011).
- [3] X.-L. Qi, T. L. Hughes, S. Raghu, and S.-C. Zhang, Time-Reversal-Invariant Topological Superconductors and Superfluids in Two and Three Dimensions, *Phys. Rev. Lett.* **102**, 187001 (2009).
- [4] X.-L. Qi and S.-C. Zhang, Topological insulators and superconductors, *Rev. Mod. Phys.* **83**, 1057 (2011).
- [5] L. Fu and C. L. Kane, Superconducting Proximity Effect and Majorana Fermions at the Surface of a Topological Insulator, *Phys. Rev. Lett.* **100**, 096407 (2008).
- [6] V. Mourik, K. Zuo, S. M. Frolov, S. R. Plissard, E. P. A. M. Bakkers, and L. P. Kouwenhoven, Signatures of Majorana fermions in hybrid superconductor-semiconductor nanowire devices, *Science* **336**, 1003 (2012).
- [7] S. M. Albrecht, A. P. Higginbotham, M. Madsen, F. Kuemmeth, T. S. Jespersen, J. Nygård, P. Krogstrup, and C. M. Marcus, Exponential protection of zero modes in Majorana islands, *Nature (London)* **531**, 206 (2016).
- [8] S. Sasaki and T. Mizushima, Superconducting doped topological materials, *Physica C (Amsterdam)* **514**, 206 (2015).
- [9] M. Sato and Y. Ando, Topological superconductors: A review, *Rep. Prog. Phys.* **80**, 076501 (2017).
- [10] Y. S. Hor, A. J. Williams, J. G. Checkelsky, P. Roushan, J. Seo, Q. Xu, H. W. Zandbergen, A. Yazdani, N. P. Ong, and R. J. Cava, Superconductivity in $\text{Cu}_x\text{Bi}_2\text{Se}_3$ and its Implications for Pairing in the Undoped Topological Insulator, *Phys. Rev. Lett.* **104**, 057001 (2010).
- [11] Y. Qiu, K. N. Sanders, J. Dai, J. E. Medvedeva, W. Wu, P. Ghaemi, T. Vojta, and Y. S. Hor, Time reversal symmetry breaking superconductivity in topological materials, [arXiv:1512.03519](https://arxiv.org/abs/1512.03519).
- [12] Z. Liu, X. Yao, J. Shao, M. Zuo, L. Pi, S. Tan, C. Zhang, and Y. Zhang, Superconductivity with topological surface state in $\text{Sr}_x\text{Bi}_2\text{Se}_3$, *J. Am. Chem. Soc.* **137**, 10512 (2015).
- [13] K. Matano, M. Kriener, K. Segawa, Y. Ando, and G.-Q. Zheng, Spin-rotation symmetry breaking in the superconducting state of $\text{Cu}_x\text{Bi}_2\text{Se}_3$, *Nat. Phys.* **12**, 852 (2016).
- [14] S. Yonezawa, K. Tajiri, S. Nakata, Y. Nagai, Z. Wang, K. Segawa, Y. Ando, and Y. Maeno, Thermodynamic evidence for nematic superconductivity in $\text{Cu}_x\text{Bi}_2\text{Se}_3$, *Nat. Phys.* **13**, 123 (2016).
- [15] T. Asaba, B. J. Lawson, C. Tinsman, L. Chen, P. Corbae, G. Li, Y. Qiu, Y. S. Hor, L. Fu, and L. Li, Rotational Symmetry Breaking in a Trigonal Superconductor Nb-doped Bi_2Se_3 , *Phys. Rev. X* **7**, 011009 (2017).
- [16] J. Y. Shen, W.-Y. He, N. F. Qi Yuan, Z. Huang, C.-W. Cho, S. H. Lee, Y. S. Hor, K. T. Law, and R. Lortz, Nematic topological superconducting phase in Nb-doped Bi_2Se_3 , *npj Quantum Mater.* **2**, 59 (2017).
- [17] M. P. Smylie, H. Claus, U. Welp, W.-K. Kwok, Y. Qiu, Y. S. Hor, and A. Snezhko, Evidence of nodes in the order parameter of the superconducting doped topological insulator $\text{Nb}_x\text{Bi}_2\text{Se}_3$ via penetration depth measurements, *Phys. Rev. B* **94**, 180510 (2016).
- [18] M. P. Smylie, K. Willa, H. Claus, A. Snezhko, I. Martin, W.-K. Kwok, Y. Qiu, Y. S. Hor, E. Bokari, P. Niraula, A. Kayani, V. Mishra, and U. Welp, Robust odd-parity superconductivity in the doped topological insulator $\text{Nb}_x\text{Bi}_2\text{Se}_3$, *Phys. Rev. B* **96**, 115145 (2017).
- [19] Y. Nagai, H. Nakamura, and M. Machida, Rotational isotropy breaking as proof for spin-polarized Cooper pairs in the topological superconductor $\text{Cu}_x\text{Bi}_2\text{Se}_3$, *Phys. Rev. B* **86**, 094507 (2012).
- [20] L. Fu, Odd-parity topological superconductor with nematic order: Application to $\text{Cu}_x\text{Bi}_2\text{Se}_3$, *Phys. Rev. B* **90**, 100509 (2014).
- [21] J. W. F. Venderbos, V. Kozii, and L. Fu, Identification of nematic superconductivity from the upper critical field, *Phys. Rev. B* **94**, 094522 (2016).
- [22] R. Joynt and L. Taillefer, The superconducting phases of UPt_3 , *Rev. Mod. Phys.* **74**, 235 (2002).
- [23] Y. Pan, A. M. Nikitin, G. K. Araizi, Y. K. Huang, Y. Matsushita, T. Naka, and A. de Visser, Rotational symmetry breaking in the topological superconductor $\text{Sr}_x\text{Bi}_2\text{Se}_3$ probed by upper-critical field experiments, *Sci. Rep.* **6**, 28632 (2016).
- [24] A. M. Nikitin, Y. Pan, Y. K. Huang, T. Naka, and A. de Visser, High-pressure study of the basal-plane anisotropy of the upper critical field of the topological superconductor $\text{Sr}_x\text{Bi}_2\text{Se}_3$, *Phys. Rev. B* **94**, 144516 (2016).
- [25] G. Du, Y. Li, J. Schneeloch, R. D. Zhong, G. Gu, H. Yang, H. Lin, and H.-H. Wen, Superconductivity with two-fold symmetry in topological superconductor $\text{Sr}_x\text{Bi}_2\text{Se}_3$, *Sci. China Phys. Mech. Astron.* **60**, 037411 (2017).
- [26] M. P. Smylie, K. Willa, H. Claus, A. E. Koshelev, K. W. Song, W. K. Kwok, Z. Islam, G. D. Gu, J. A. Schneeloch, R. D. Zhong, and U. Welp, Superconducting and normal-state anisotropy of the doped topological insulator $\text{Sr}_{0.1}\text{Bi}_2\text{Se}_3$, *Sci. Rep.* **8**, 7666 (2018).
- [27] S. Tagliati, V. M. Krasnov, and A. Rydh, Differential membrane-based nanocalorimeter for high-resolution measurements of low-temperature specific heat, *Rev. Sci. Instrum.* **83**, 055107 (2012).
- [28] K. Willa, Z. Diao, D. Campanini, U. Welp, R. Divan, M. Hudl, Z. Islam, W.-K. Kwok, and A. Rydh, Nanocalorimeter platform for *in situ* specific heat measurements and x-ray diffraction at low temperature, *Rev. Sci. Instrum.* **88**, 125108 (2017).
- [29] H. Leng, D. Cherian, Y. K. Huang, J.-C. Orain, A. Amato, and A. de Visser, Muon spin rotation study of the topological superconductor $\text{Sr}_x\text{Bi}_2\text{Se}_3$, *Phys. Rev. B* **97**, 054503 (2018).
- [30] A. Rutgers, Note on supraconductivity, *Physica* **1**, 1055 (1934).
- [31] P. G. De Gennes, *Superconductivity of Metals and Alloys* (West View Press, Boulder, CO, 1966).
- [32] J. Bardeen, L. N. Cooper, and J. R. Schrieffer, Theory of superconductivity, *Phys. Rev.* **108**, 1175 (1957).
- [33] Shruti, V. K. Maurya, P. Neha, P. Srivastava, and S. Patnaik, Superconductivity by Sr intercalation in the layered topological insulator Bi_2Se_3 , *Phys. Rev. B* **92**, 020506 (2015).
- [34] D. F. Agterberg and M. B. Walker, Ginzburg-Landau model of hexagonal superconductors: Application to UPt_3 , *Phys. Rev. B* **51**, 8481 (1995).
- [35] D. F. Agterberg and M. B. Walker, Theory for the Angular Dependence of the Upper Critical Field of Superconducting UPt_3 , *Phys. Rev. Lett.* **74**, 3904 (1995).
- [36] See Supplemental Material at <http://link.aps.org/supplemental/10.1103/PhysRevB.98.184509> for a detailed analysis on the upper critical field .

- [37] R. A. Fisher, S. Kim, B. F. Woodfield, N. E. Phillips, L. Taillefer, K. Hasselbach, J. Flouquet, A. L. Giorgi, and J. L. Smith, Specific Heat of UPt_3 : Evidence for Unconventional Superconductivity, *Phys. Rev. Lett.* **62**, 1411 (1989).
- [38] B. Bogenberger, H. Löhneysen, T. Trappmann, and L. Taillefer, Phase diagram of superconducting UPt_3 by the magnetocaloric effect, *Physica B (Amsterdam)* **186–188**, 248 (1993).
- [39] D. S. Jin, S. A. Carter, B. Ellman, T. F. Rosenbaum, and D. G. Hinks, Uniaxial-Stress Anisotropy of the Double Superconducting Transition in UPt_3 , *Phys. Rev. Lett.* **68**, 1597 (1992).
- [40] K. Hasselbach, L. Taillefer, and J. Flouquet, Critical Point in the Superconducting Phase Diagram of UPt_3 , *Phys. Rev. Lett.* **63**, 93 (1989).
- [41] M. Sigrist and K. Ueda, Phenomenological theory of unconventional superconductivity, *Rev. Mod. Phys.* **63**, 239 (1991).
- [42] S. K. Yip, T. Li, and P. Kumar, Thermodynamic considerations and the phase diagram of superconducting UPt_3 , *Phys. Rev. B* **43**, 2742 (1991).
- [43] M. Boukhny, G. L. Bullock, and B. S. Shivaram, Thermodynamics of superconducting UPt_3 under uniaxial pressure, *Phys. Rev. B* **50**, 8985 (1994).